Global and Planetary Change 151 (2017) 68–79

Contents lists available at ScienceDirect

Global and Planetary Change

journal homepage: www.elsevier.com/locate/gloplacha

Anomalies of the upper water column in the Mediterranean Sea

Irene Rivetti [a,*], Ferdinando Boero [a,b,d], Simonetta Fraschetti [a], Enrico Zambianchi [c,e], Piero Lionello [a,b]

[a] Dipartimento di Scienze e Tecnologie Biologiche ed Ambientali, Università del Salento, CoNISMa, 73100 Lecce, Italy
[b] CMCC Euro-Mediterranean Center on Climate Change, 73100 Lecce, Italy
[c] Dipartimento di Scienze per l'Ambiente, Università degli Studi di Napoli "Parthenope", CoNISMa, 80143 Napoli, Italy
[d] Istituto di Scienze Marine del CNR, 16149 Genova, Italy
[e] Istituto di Scienze dell'Atmosfera e del Clima del CNR, 00133 Roma, Italy

ARTICLE INFO

Article history:
Received 14 July 2015
Received in revised form 19 January 2016
Accepted 1 March 2016
Available online 3 March 2016

Keywords:
Mixed layer
Seasonal thermocline
Mass mortalities
Temperature profiles
Benthic invertebrates
Mediterranean Sea

ABSTRACT

The evolution of the upper water column in the Mediterranean Sea during more than 60 years is reconstructed in terms of few parameters describing the mixed layer and the seasonal thermocline. The analysis covers the period 1945–2011 using data from three public sources: MEDAR-MEDATLAS, World Ocean Database, MFS-VOS program. Five procedures for estimating the mixed layer depth are described, discussed and compared using the 20-year long time series of temperature profiles of the DYFAMED station in the Ligurian Sea. On this basis the so-called three segments profile model (which approximates the upper water column with three segments representing mixed layer, thermocline and deep layer) has been selected for a systematic analysis at Mediterranean scale. A widespread increase of the thickness and temperature of the mixed layer, increase of the depth and decrease of the temperature of the thermocline base have been observed in summer and autumn during the recent decades. It is shown that positive temperature extremes of the mixed layer and of its thickness are potential drivers of the mass mortalities of benthic invertebrates documented since 1983. Hotspots of mixed layer anomalies have been also identified. These results refine previous analyses showing that ongoing and future warming of upper Mediterranean is likely to increase mass mortalities by producing environmental conditions beyond the limit of tolerance of some benthic species.

1. Introduction

The mixed layer (ML) depth is one of the most important upper ocean variables. Its variations influence the volume of water over which the surface heat flux is distributed (Chen et al., 1994; Ohlmann et al., 1996) and the vertical distribution of biological, chemical and particulate components (Gardner et al., 1995). Many studies emphasize its key role in physical and biological processes (e.g., Kara et al., 2003; de Boyer Montègut et al., 2004; Zawada et al., 2005, Bindoff et al., 2007). Recently, Dong et al. (2009) suggested that a proper representation of the temporal variation of the ML depth (MLD) is required for an accurate upper ocean thermal balance as heat storage and release strongly depend on it. Several authors show that processes in the MLD influence the sea surface temperature (SST) variability, so that an accurate MLD representation is important to predict SST anomalies on seasonal and longer time scales (Deser et al., 1996; Alexander et al., 2001; Dommenget and Latif, 2002; Hanawa and Sugimoto, 2004). For the marine environment MLD is an ecological boundary, because it represents the level of the physiological temperature limit for many species and nutrients, oxygen, and other limiting factors tend to accumulate near it (Polovina et al., 1995; Babu et al., 2004; Yasuda and Watanabe, 2007).

In the absence of direct measurements of both turbulence and mixing, MLD is commonly estimated from temperature or density profile data by using simple numerical schemes, which, however, may lead to different values. Various studies (Monterey and Levitus, 1997; Kara et al., 2003) underline the difficulty in establishing an objective and general criterion for defining adequately the MLD from hydrographic profiles. The complexity of observed temperature profiles, due to the presence of multiple gradients, temperature inversions and measurement noise, can make the identification of the ML and estimate of the MLD uncertain, both by objective computer algorithms and by visually (and subjectively) examining individual profiles.

The threshold method and the gradient method are widely used and simple procedures for finding MLD. The threshold method considers the temperature decrease (or the density increase) along the profile beyond an initial reference level and estimates the MLD as the depth at which it crosses a predefined value (e.g., de Boyer Montègut et al., 2004; Suga

Abbreviations: ML, mixed layer; MLD, mixed layer depth; MLT, mixed layer temperature; TBD, thermocline base depth; TBT, thermocline base temperature; THR, threshold method; CUR, curvature-based criterion; 3SEG, three segments profile model; SM, split and merge algorithm; ISO, variable representative isotherm method; VIS, visual estimate.

* Corresponding author at: Dept. of Biological and Environmental Sciences and Technology, University of Salento, I-73100 Lecce, Italy.
E-mail address: irene.rivetti@unisalento.it (I. Rivetti).

http://dx.doi.org/10.1016/j.gloplacha.2016.03.001
0921-8181/

et al., 2004). Analogously, the gradient method searches for the depth at which the temperature (density) gradient reaches a predefined threshold (e.g., Monterey and Levitus, 1997). These methods depend on predefined thresholds and reference depth values, which are very difficult to be univocally determined for all different hydrographic profiles (Kara et al., 2000; Lorbacher et al., 2006; Holte and Talley, 2009).

Other procedures search for the best fit of the temperature or density profile to a predefined "ideal" functional form, which consists in a set of linear or non-linear functions with different degrees of complexity, involving two segments (Freeland, 2013), an undefined number of segments (Thomson and Fine, 2003), and nonlinear functions (e.g. Chu et al., 1997). The main advantage of these approximations is that, beside the MLD, they can give information on other parameters of the profile, such as the thermocline temperature gradient and its extension.

Another alternative procedure uses representative isotherms as proxy for thermocline parameters, such as the MLD and the thermocline base depth (TBD) (Pizarro and Montecinos, 2004). The chosen isotherm level varies in the literature. Past studies have used the 20 °C isotherm (Donguy and Meyers, 1987; Kessler, 1990; Kessler et al., 1995), the 14 °C isotherm (Meyers, 1979a, 1979b; Sharp and McLain, 1993) and the 12 °C isotherm (Wang et al., 2000).

In the Mediterranean Sea, several works have produced estimates of the MLD from hydrographic temperature profiles. Among these, D'Ortenzio et al. (2005) produced a monthly MLD climatology (0.5° resolution) by using the threshold method based on a temperature decrease of 0.02 °C from the near-surface value at 10 m depth. Other works have considered the temporal evolution of the MLD for studies on phytoplankton phenology (Vidussi et al., 2001; Bernardello et al., 2012; Lavigne et al., 2013), vertical export flux dynamics (Heimburger et al., 2013), carbon fluxes in the mixed layer (D'Ortenzio et al., 2008; Taillandier et al., 2012) and the performance of mixing model (Kara et al., 2010; Ruiz et al., 2012). In all these works, the threshold method has been used for MLD detection.

Studies on mass mortalities of benthic invertebrates in the Mediterranean Sea emphasize that positive thermal anomalies of the upper water column trigger these events. Further, mass mortalities that occurred in 1993, 1999 and 2008 were directly associated to sudden deepening of the ML (e.g., Cerrano et al., 2000; Linares et al., 2005; Coma et al., 2009; Garrabou et al., 2009; Bensoussan et al., 2010; Cebrian et al., 2011; Huete-Stauffer et al., 2011; Rivetti et al., 2014).

This study describes the temporal evolution of selected parameters (the MLD, the ML Temperature (MLT), the TBD and the TB Temperature (TBT)) in the whole Mediterranean Sea, for the period 1945–2011. Five procedures for determining the MLD have been analyzed and compared on hydrographic temperature profiles collected at DYFAMED station. Agreement and disagreement among procedures and with the visual estimate of MLD have been discussed and the three segments profile model (see Section 2.2. and Appendix A) has been applied to all hydrographic temperature profiles available in the basin. Finally, the effect of the MLD and of the MLT on the mass mortality events of benthic invertebrates documented in the basin has been evaluated. Recently Rivetti et al. (2014) showed that documented mass mortalities are consistent with positive temperature trends at basin scale, with atypical thermal conditions registered at the smaller spatial and temporal scale of mass mortality events. This study deepens that analysis, focusing the attention on the above-mentioned selected parameters characterizing the vertical temperature profile of the upper water column.

The data used in this study are described in Section 2.1. Five procedures for the analysis of the vertical temperature profile are then discussed and compared in Section 2.2. Differences among them have been evaluated and the most suitable procedure to capture ML characteristics has been chosen for subsequent analysis. In Section 3, trends of selected thermocline parameters are presented for winter (January, February, March), spring (April, May, June), summer (July, August, September) and autumn (October, November, December) by using all hydrographic temperature profiles available in the Mediterranean Sea for the period 1945–2011. In Section 4, the link between the ML characteristics and documented mass mortalities of benthic invertebrates in the locations and periods in which these events occurred is evaluated and discussed. Further, this section compares ML anomalies in the first and last parts of the time series both in the locations and months where mortalities have been reported and for the whole Mediterranean Sea in summer and autumn. Section 5 draws the conclusions of this study. A detailed description of the five procedures used to estimate the MLD is given in Appendix A. Appendix B describes an example of application of the selected procedure considering the time series of summer temperature profiles at the DYFAMED station.

2. Materials and methods

2.1. Data sources

2.1.1. The DYFAMED station temperature profiles

In our study, 5 procedures for ML analysis have been compared by applying them to the temperature profiles collected with digital Conductivity Temperature Depth (CTD) at DYFAMED station (Fig. 1). The site is located 52 km off Cape Ferrat, at 43°25′N, 07°52′E in the Ligurian Sea, Western Mediterranean Sea. The DYFAMED station contributes to the Mediterranean Ocean Observing System on Environment (MOOSE) and to the activities of the HYDROCHANGES group. Its data are available through the EuroSITES (European Ocean Observatory Network) website (http://www.eurosites.info/dyfamed.php). The temperature profiles cover the period from January 1991 to December 2009. In this study, DYFAMED time-series has been linearly interpolated at 1 m resolution. These data are particularly valuable for climatic studies because the sampling protocol has remained unchanged since the beginning of the program, so that they are continuous and homogeneous in time.

2.1.2. Temperature profiles in the Mediterranean Sea

Temperature profiles contained in MEDAR/MEDATLAS (Fichaut et al., 2003), the largest historical database of hydrographic variables collected in the Mediterranean and Black Sea, have been used in

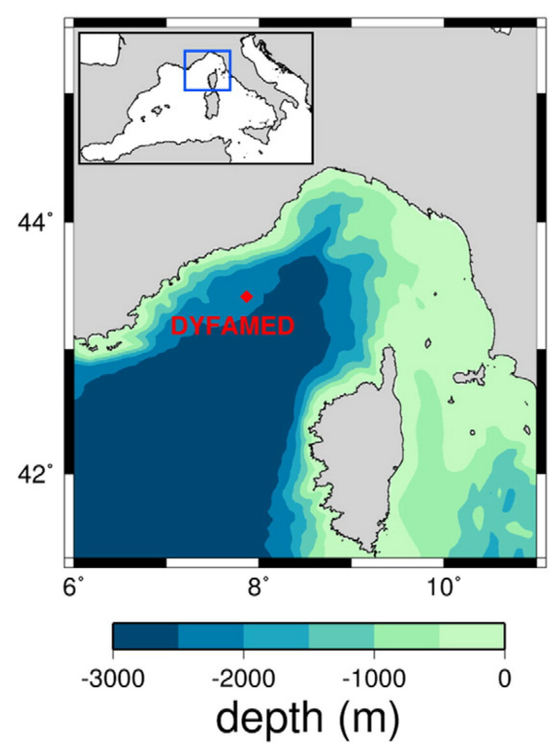

Fig. 1. Map of the Ligurian Sea with the location of the DYFAMED station.

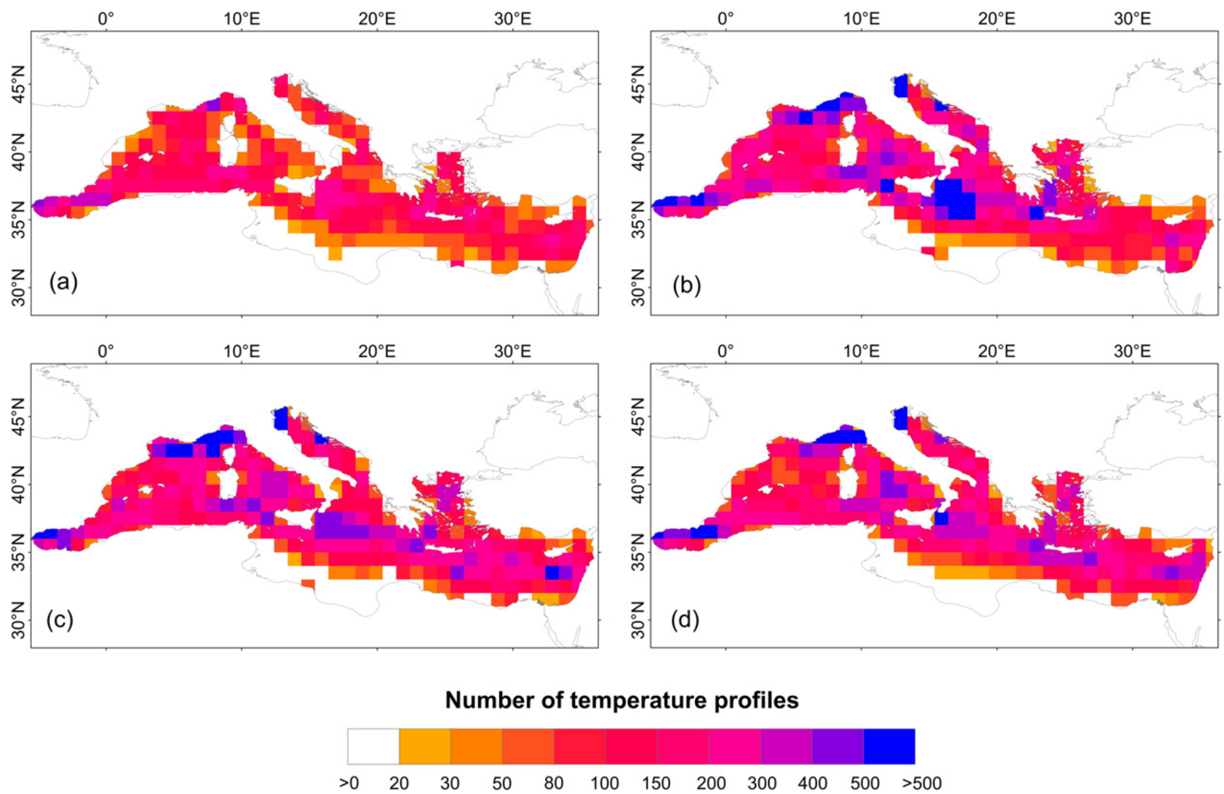

Fig. 2. Spatial distribution of the number of temperature profiles. Colors show the number of observations in each 1° lat × 1° lon cell for the period 1945–2011 in winter (a), in spring (b), in summer (c) and in autumn (d).

this study. Data range from 1889 to 2000 and were collected with bottles, Mechanical Bathy-Thermographs (MBT), eXpendable Bathy-Thermographs (XBT), and Conductivity–Temperature–Depth (CTD). MEDAR/MEDATLAS profiles have been integrated with two other datasets: CTD and XBT data (covering the period 2000–2013) of the *World Ocean Database 2013* (WOD13) (Johnson et al., 2013) and XBT measurements (covering the period 1999–2011) of the Mediterranean Forecasting System-Voluntary Observing Ship program (MFS-VOS) (Manzella et al., 2007).

Our analysis is focused on the period 1945–2011 (because before 1945 and after 2011 data are sparsely and irregularly available) and on winter, spring, summer and autumn. The appraisal of the distribution

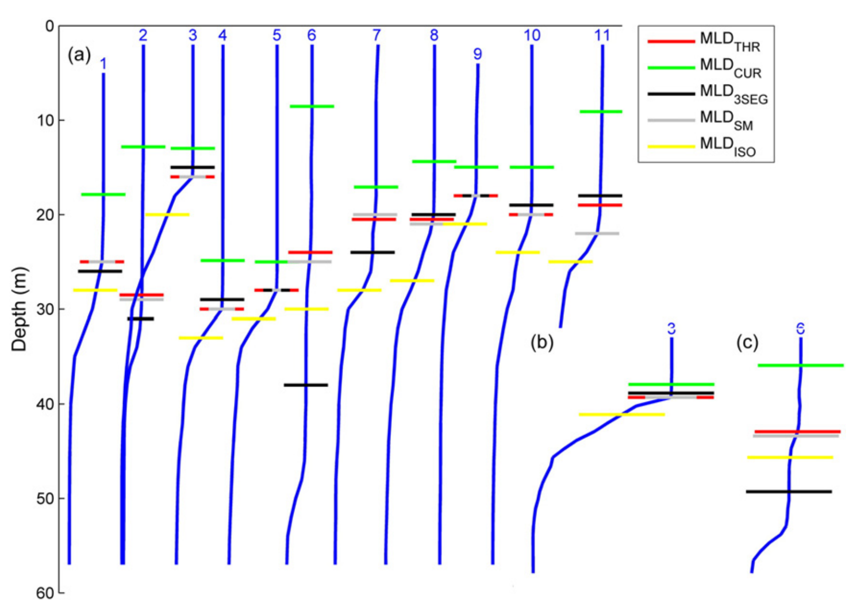

Fig. 3. Temperature profiles from randomly chosen CTD casts collected at DYFAMED station (a), a temperature profile with a well-defined mixed layer (b), and with multiple temperature steps (c). The vertical scale of (b) and (c) (corresponding to profile numbers 3 and 6 in (a)) has been deformed for graphical convenience. Horizontal bars denote MLD derived using the threshold method (MLD_{THR}), the curvature-based criterion (MLD_{CUR}), the three segments profile model (MLD_{3SEG}), the split and merge algorithm (MLD_{SM}) and the variable representative isotherm method (MLD_{ISO}).

Table 1
Statistics of MLDs computed among procedures (MLD_{THR}, MLD_{CUR}, MLD_{3SEG}, MLD_{SM}, MLD_{ISO}) and with respect to the subjective estimate (MLD_{VIS}). Values are based on 246 CTD casts collected at DYFAMED station. Columns report for each procedure the Pearson's correlation coefficient (r), bias and the standard deviation (std). The first column reports the percentage of cases where the MLD has been identified.

		MLD_{VIS}			MLD_{THR}			MLD_{CUR}			MLD_{3SEG}			MLD_{SM}			MLD_{ISO}		
	% of MLDs	r	Bias (m)	std (m)	r	Bias (m)	std (m)	r	Bias (m)	std (m)	r	Bias (m)	std (m)	r	Bias (m)	std (m)	r	Bias (m)	std (m)
MLD_{VIS}	94.31%	1.00	0.00	0.00	0.67	−2.17	12.67	0.45	−7.55	16.29	0.84	−5.34	8.55	0.73	−6.60	10.86	0.87	3.36	4.48
MLD_{THR}	95.93%	0.67	2.17	12.67	1.00	0.00	0.00	0.75	−9.69	26.92	0.60	−6.53	28.94	0.17	−9.46	35.79	0.77	4.72	5.70
MLD_{CUR}	100.00%	0.45	7.55	16.29	0.75	9.69	26.92	1.00	0.00	0.00	0.47	1.42	25.63	0.22	−2.02	28.18	0.69	7.87	6.50
MLD_{3SEG}	100.00%	0.84	5.34	8.55	0.60	6.53	28.94	0.47	−1.42	25.63	1.00	0.00	0.00	0.62	−3.43	14.43	0.76	6.32	5.87
MLD_{SM}	100.00%	0.73	6.60	10.86	0.17	9.46	35.79	0.22	2.02	28.18	0.62	3.44	14.43	1.00	0.00	0.00	0.68	6.41	6.59
MLD_{ISO}	68.29%	0.87	−3.36	4.48	0.77	−4.72	5.70	0.69	−7.87	6.50	0.76	−6.32	5.87	0.68	−6.42	6.59	1.00	0.00	0.00

of temperature along the water column and its evolution in time requires a careful quality control of individual profiles, which is extensively described in Rivetti et al. (2014). Out of 249,687 analyzed temperature profiles available in the period 1945–2011, 53,857 were discarded after the quality control. The remaining 195,830 profiles have been linearly interpolated at 1 m intervals in depth before being analyzed.

The pattern of data distribution (Fig. 2) is fairly similar across seasons, though winter is slightly less sampled for logistical and meteorological reasons. The lowest number of observations was collected along the coasts of Tunisia, Libya and Egypt; the highest density of observations was found in the Liguro-Provençal sub basin, in the Alboran Sea, in the central Ionian Sea and in the North Adriatic Sea.

2.1.3. Mass mortalities of marine benthic invertebrates

In this study, we consider the same 19 events that have been extracted from 34 published studies described in Rivetti et al. (2014), reporting mass mortalities for 59 species across the Mediterranean Sea. This study show that the first documented mass mortality event occurred in 1983 in the Ligurian Sea and their frequency steadily increased since the year 1992. In addition, most mortalities occurred in the first 30 m in late summer–early fall, have been reported in the Western Mediterranean and cnidarians and sponges were the most affected taxa.

2.2. Procedures for MLD analysis and their intercomparison

Due to the scarcity of available density profiles, only temperature profiles are considered in this study to estimate the MLD (as discussed by D'Ortenzio et al., 2005).

The five procedures considered are: the threshold method (THR), the curvature-based criterion (CUR), the three segments profile model (3SEG), the split and merge algorithm (SM) and the variable representative isotherm method (ISO). A detailed description of these procedures is given in Appendix A (Table A.1). The visual estimate (VIS) has

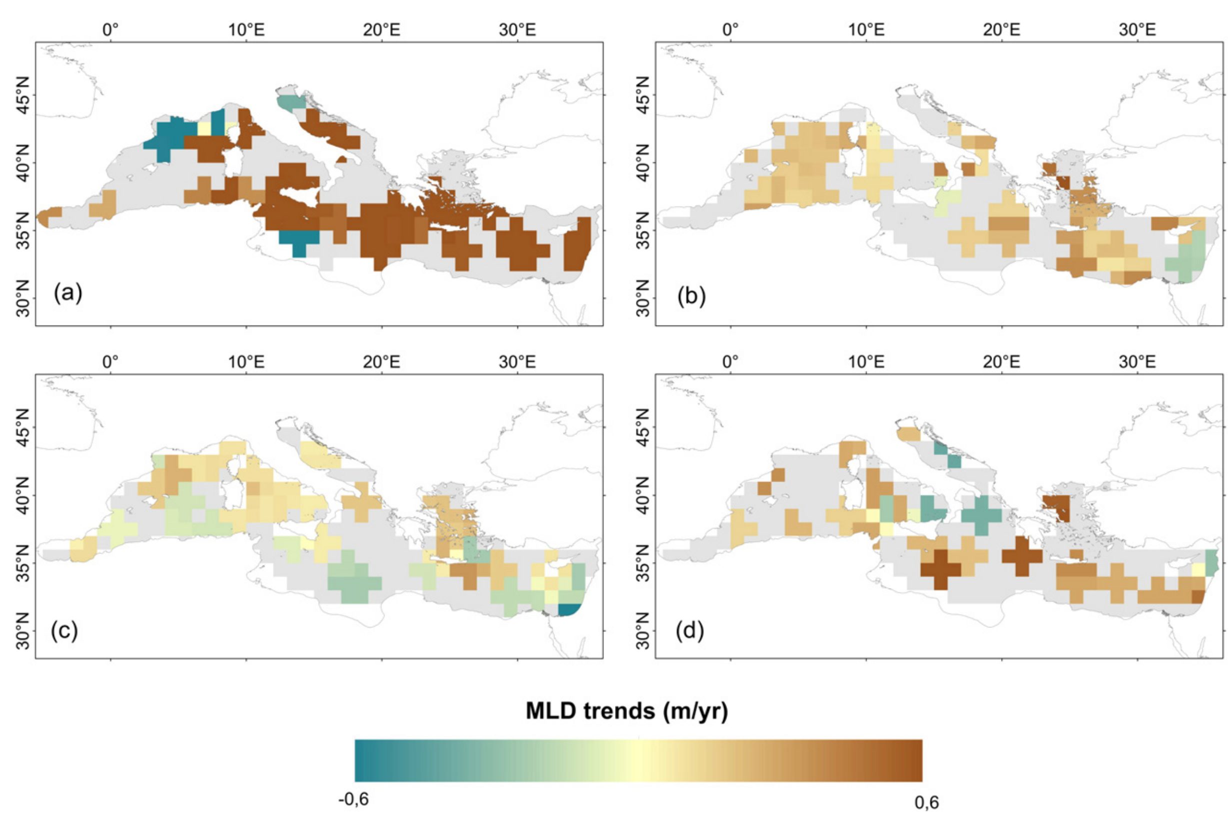

Fig. 4. MLD trends (m/year) in winter (a), spring (b), summer (c) and autumn (d) for the period 1945–2011. Linear regressions have been calculated for cells of 1° latitude by 1° longitude and tested for statistical significance at the 90% confidence level. Significant increased/decreased MLD trends are reported as colored cells, not significant increased/decreased MLD trends are reported as gray areas. Areas without sufficient data are left white.

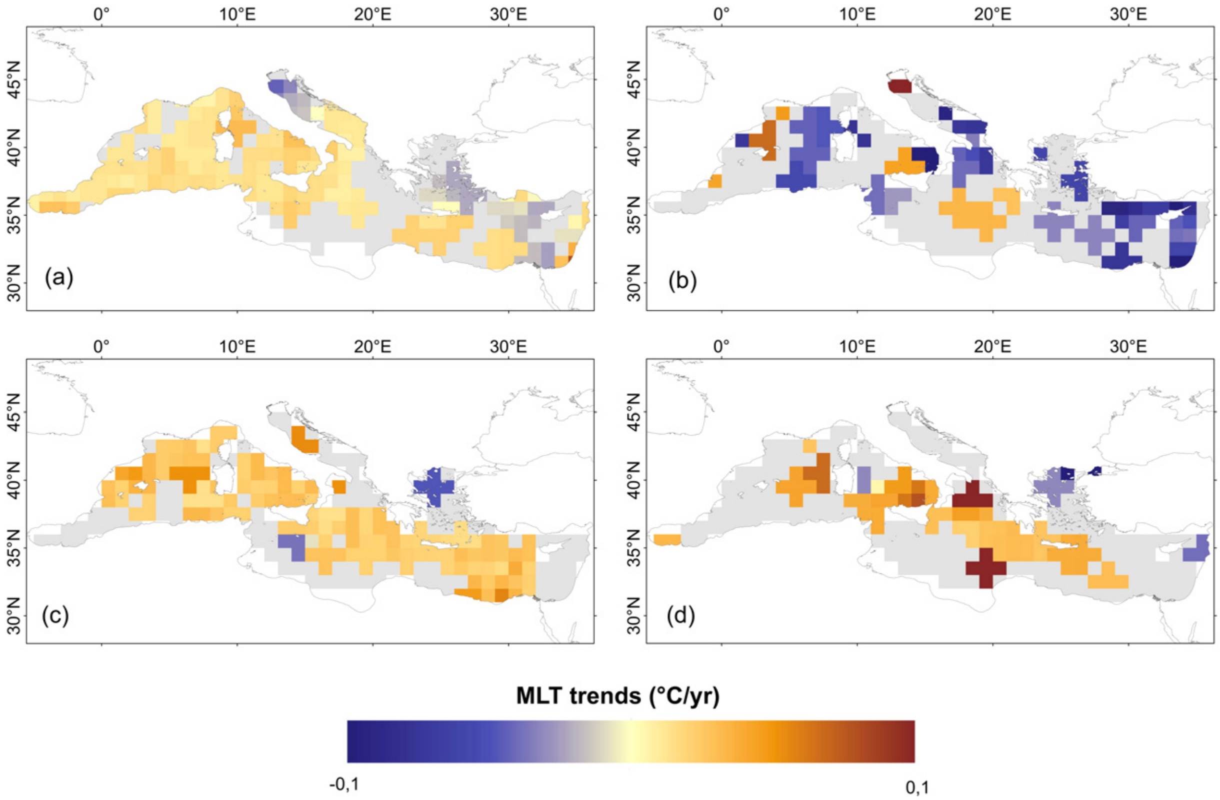

Fig. 5. Same as Fig. 4, except it shows MLT trends.

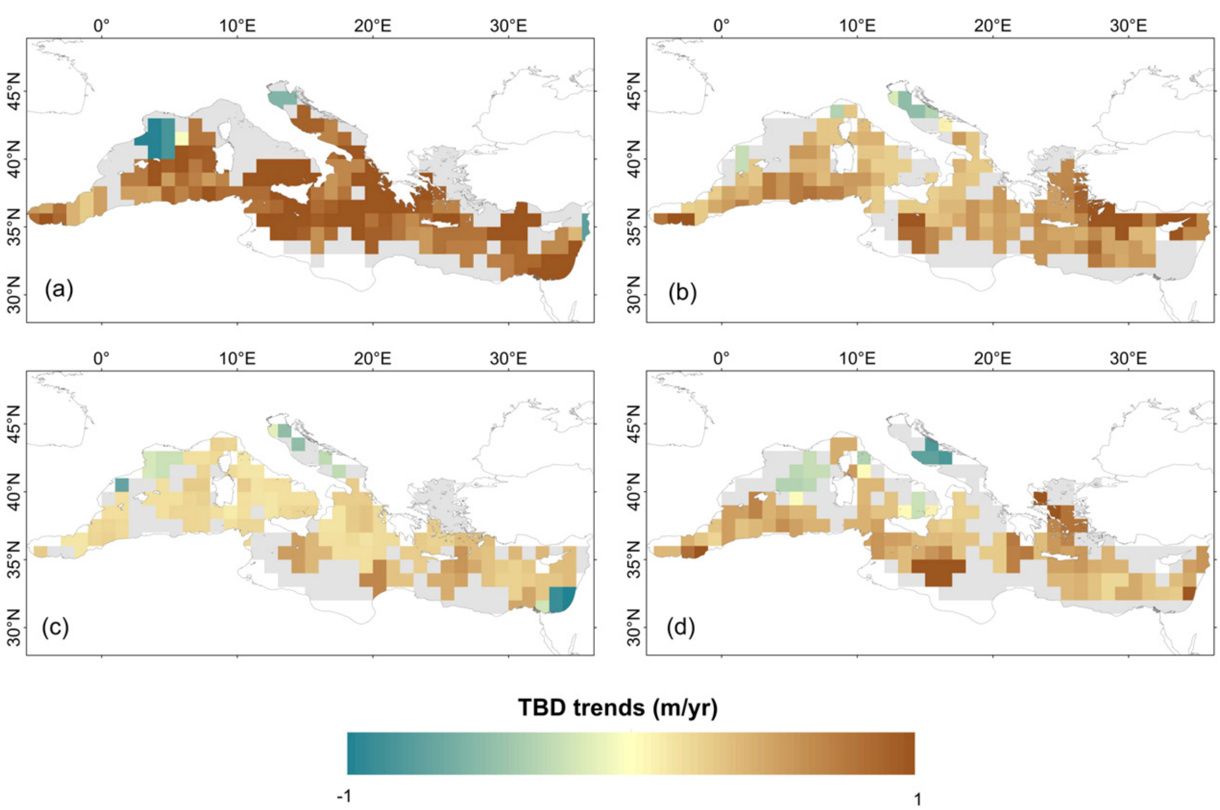

Fig. 6. Same as Fig. 4, except it shows TBD trends.

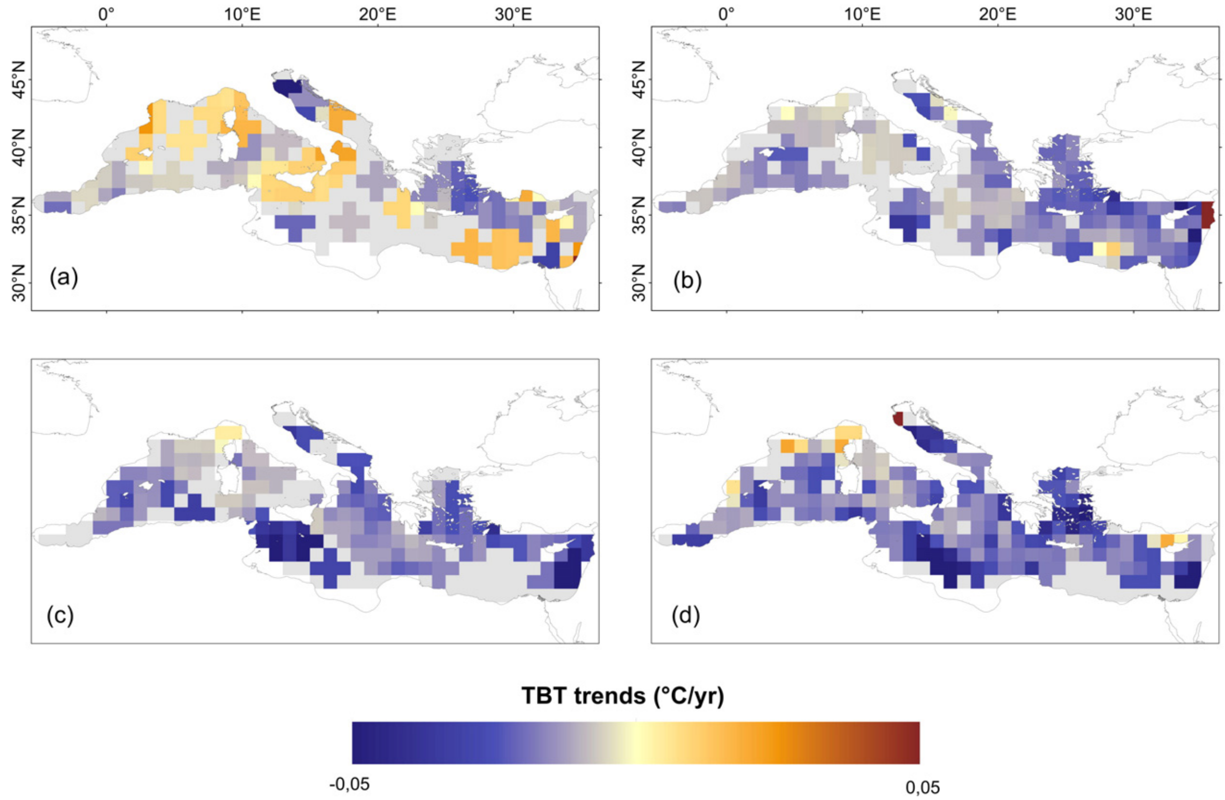

Fig. 7. Same as Fig. 4, except it shows TBT trends.

been based on the subjective identification of the step marking the basis of the ML, which is obviously depending on a personal judgment and has an uncertainty, whose assessment is however beyond the scope of this paper.

Temperature profiles collected at the DYFAMED station have been analyzed visually and using the five considered procedures. The resulting MLDs have been intercompared. Fig. 3 shows MLD estimates (horizontal line segments) for a set of randomly selected profiles. In general (Fig. 3a and Table 1), CUR leads to smaller MLD values compared to other algorithms, confirming the results of Lorbacher et al. (2006). On the contrary, ISO usually produces a thicker MLD than the other procedures. When the upper water column has a uniform temperature and is clearly delimited by a well-defined thermocline (Fig. 3b), THR, 3SEG, and SM provide nearly identical MLD values. When the upper water column presents multiple layers connected by small transitions (Fig. 3c), results depend strongly on the procedure. In this case,

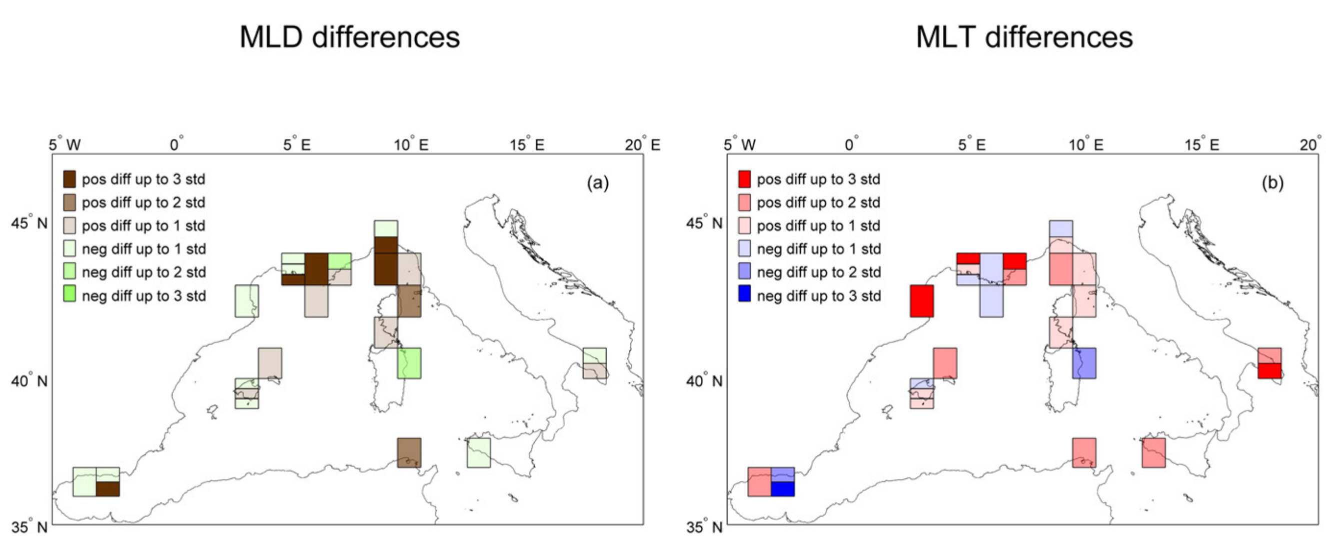

Fig. 8. MLD (a) and MLT (b) differences with respect to the local mean value during mass mortality events. Brown/green rectangles show that the MLD during mass mortality events was deeper/shallower than the mean MLD over the period 1945–2011. Red/blue rectangles show that the MLT during mass mortality events was higher/lower than the mean MLT over the period 1945–1982. Some rectangles are divided into several parts because in those locations more of one mass mortality event occurred. Pale, medium, strong colors are used for denoting differences in the range up to 1, 2, and 3 standard deviations (std) as annotated in the upper left corner of each panel.

there is no well-defined ML, and producing a convincing MLD estimate is difficult for all algorithms. Fig. 3 and Table 1 show that CUR identifies a shallow ML with respect to other procedures and suggests that 3SEG matches well the MLD visual estimate.

Table 1 compares the MLD values produced by each algorithm (MLD_{THR}, MLD_{CUR}, MLD_{3SEG}, MLD_{SM}, MLD_{ISO}) and the subjective estimate obtained by visual inspection of the profiles (MLD_{VIS}). It reports correlation coefficient (r), bias and standard deviation (std) among the procedures and the subjective estimate MLD_{VIS} considering 246 temperature profiles from spring to autumn (winter profiles have not been included in this analysis). When comparing the MLD procedures to the subjective estimate (MLD_{VIS}), positive (negative) bias denotes overestimation (underestimation) and the standard deviation provides a measure of their accuracy (Holte and Talley, 2009).

Std and bias between procedures show that their MLD estimates often differ appreciably. However, MLD estimates by some procedures are well correlated, particularly MLD_{THR} and MLD_{CUR} ($r = 0.75$), MLD_{THR} and MLD_{ISO} ($r = 0.77$), MLD_{3SED} and MLD_{ISO} ($r = 0.76$). Considering the comparison against the visual estimate, MLD_{SM} presents the lowest agreement ($r = 0.45$), while MLD_{3SEG} ($r = 0.84$) and MLD_{ISO} ($r = 0.88$) appears to be particularly reliable.

MLD_{ISO} is reasonably well correlated with all other MLD estimates, suggesting that it could be used to provide the value representing a consensus among procedures, but it presents some limitations. It systematically overestimates MLD with respect to other algorithms and to MLD_{VIS} (all other procedures underestimate it, with the CUR and the SM algorithms generally producing the shallowest MLD) and it has the lowest percentage of valid MLD estimates (68.29%). On the contrary, the 3SEG method is extremely robust with a nil rate of failure and it has the highest correlation, second smallest standard deviation (after ISO) and a relatively small bias with respect to MLD_{VIS}. Therefore the 3SEG method has been used for the analysis at basin scale in our study. Appendix B shows an example with the application of the 3SEG to the summer profiles collected at the DYFAMED station.

3. Multi-decadal evolution of the upper water column

To provide an overall picture of the evolution of the stratification of the upper water column across the Mediterranean Sea over the period 1945–2011, key parameters of thermocline have been selected and linear trends have been mapped (Figs. 4–7). The 3SEG method has been applied to individual temperature profiles for estimating MLD, MLT, TBD and TBT. The analysis has considered linear regressions of each parameter on yearly basis adopting 1° latitude by 1° longitude cells. Only values that are statistically significant at the 90% level are reported as colored cells, while gray cells denote not significant values. In the white cells (mostly along the coast of Libya) there are no sufficient data for estimating trends (to estimate the trend at least 10 years of measurements have been required).

Fig. 4 shows the spatial distribution of linear trends of the MLD. In all seasons significant MLD trends are mostly positive suggesting a general deepening of the ML. This signal is more evident in winter (Fig. 4a) with trends of 0.6 m/yr for a large fraction of the basin. Scattered signals of decreasing MLD are present in the Gulf of Lion in winter (Fig. 4a), in the eastern portion of the Levantine Sea in spring (Fig. 4b), in the southern portion of the Algerian, Ionian and Levantine Seas in summer (Fig. 3c) and in the Ionian and South Tyrrhenian Seas in autumn (Fig. 4d).

Fig. 5 shows the spatial distribution of linear trends of the MLT. Cooling of the ML is dominant in spring with the exceptions of the Ionian and Balearic Seas (Fig. 5b), whereas warming occurs in almost all basin in winter and summer (Fig. 5a, c) and for the central

Table 2
Frequency of cases in which mass mortalities occurred when the MLD/MLT was higher/lower than the MLD/MLT mean values in the reference period 1945–1982. Columns with MLD+/MLD− include cases with MLD higher/lower than the MLD reference mean, rows with MLT+/MLT− include cases with MLT higher/lower than the MLT mean values.

	MLD+	MLD−	
MLT+	38.4%	30.8%	69.2%
MLT−	15.4%	15.4%	30.8%
	53.8%	46.2%	100%

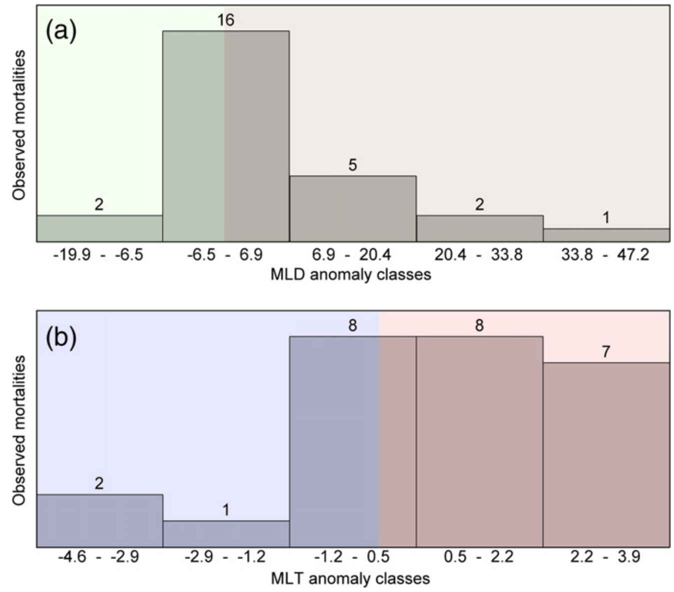

Fig. 9. Distribution of observed mortalities as function of MLD anomaly (a) and MLT anomaly (b). In Fig. 9a the green/brown background corresponds to negative/positive MLD anomalies. In Fig. 9b the blue/red background corresponds to negative/positive MLT anomalies.

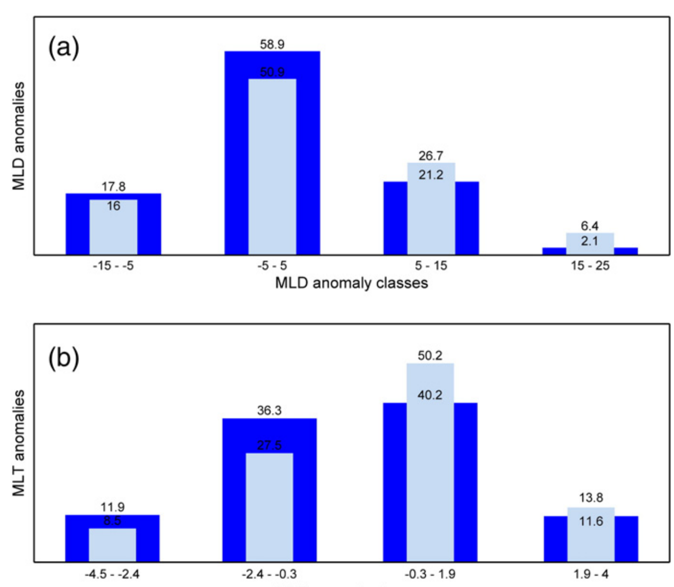

Fig. 10. Panel a shows the distribution of MLD anomalies for the periods 1945–1965 (dark blue) and 1990–2011 (light blue). Panel b shows the same information except it considers MLT. MLD/MLT anomalies have been calculated only in the locations and months where mortalities have been reported. Anomalies are with respect to the mean values in the reference period (1945–1982).

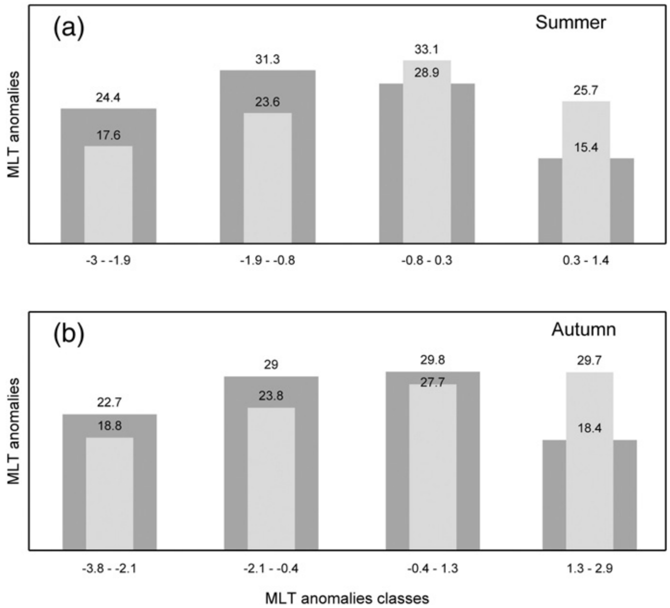

Fig. 11. Distribution of MLT anomalies for the periods 1945–1965 (dark gray) and 1990–2011 (light gray) for summer (a) and autumn (b). MLT anomalies have been calculated considering the whole Mediterranean Sea.

Mediterranean Sea in autumn (Fig. 5c), with the exception of a cooling in the Aegean Sea, occurring in all these three seasons.

Fig. 6 shows the spatial distribution of linear trends of the TBD. In all seasons significant TBD trends are mostly positive suggesting a general deepening of the TB. This signal is more evident in winter and spring (Fig. 6a, b) with trends of 1 m/yr for almost all basin. Exceptions to this positive trend are the Gulf of Lion in winter (Fig. 6a), the North Adriatic Sea in spring (Fig. 6b), the Adriatic Sea and the Gulf of Lion in summer (Fig. 6c) and the central Adriatic Sea in autumn (Fig. 6d).

Fig. 7 shows the spatial distribution of linear trends of the TBT. The TBT trends are negative over the whole basin in spring, summer and autumn, with very isolated and sparse exceptions, such as in the Ligurian Sea in summer and in autumn (Fig. 7c, d). In winter, such a clear signal has not been observed (Fig. 7a).

4. Effects of mixed layer depth and temperature on mass mortality events in the Mediterranean Sea

For each mass mortality event, MLD and MLT have been estimated considering a 3-month long period centered on the month of the event for a cell of 1° latitude by 1° longitude including the location where mass mortality occurred. These values are compared to the corresponding mean MLD and MLT over the "reference" period 1945–1982, in which mass mortalities have not been reported. The comparison is meant to provide an indication whether there is consistency between changes of the structure of the upper water column and mass mortalities. Unfortunately, temperature observations are too sparse and irregularly distributed both in time and space for adopting a narrower time window and smaller cell size than those used for these estimates, the MLD and MLT. However, the thermal inertia of the water column is expected to allow to consider the computed values as representative of the condition associated to mass mortalities events.

For each location where a mass mortality was recorded, Fig. 8 shows the corresponding MLD (Fig. 8a) and MLT (Fig. 8b) conditions. In Fig. 8a, brown/green boxes indicate that MLD was thicker/shallower than the local mean value in the reference period. Pale, medium, strong colors are used for denoting differences in the range up to 1, 2, and 3 standard deviations. Analogous information is shown in Fig. 8b, using red/blue colors to denote MLT higher/lower than the local mean value in the reference period.

This information is summarized in Table 2, which shows the frequency of cases when, in correspondence with a mass mortality, the MLD and the MLT were higher/lower than their mean value in the reference period. Most mass mortalities occurred when the MLT was higher than the reference value (69.2%). Among these 38.4% occurred when MLD was thicker and 30.8% occurred when MLD was shallower than the reference period mean values. This suggests that warm MLT anomalies are associated with mass mortalities, while MLD exerts a lower influence.

The relationship between the occurrences of mass mortalities and the MLD/MLT anomalies with respect to the reference period has been further assessed through the Kolmogorov–Smirnov test (KS-test; Lopes, 2011). The test was performed comparing the observed distribution of mass mortalities with the uniform distribution. Evenly sized MLD/MLT anomaly intervals have been adopted. If MLD and MLT had no influence on mass mortalities the distribution of the observed mass

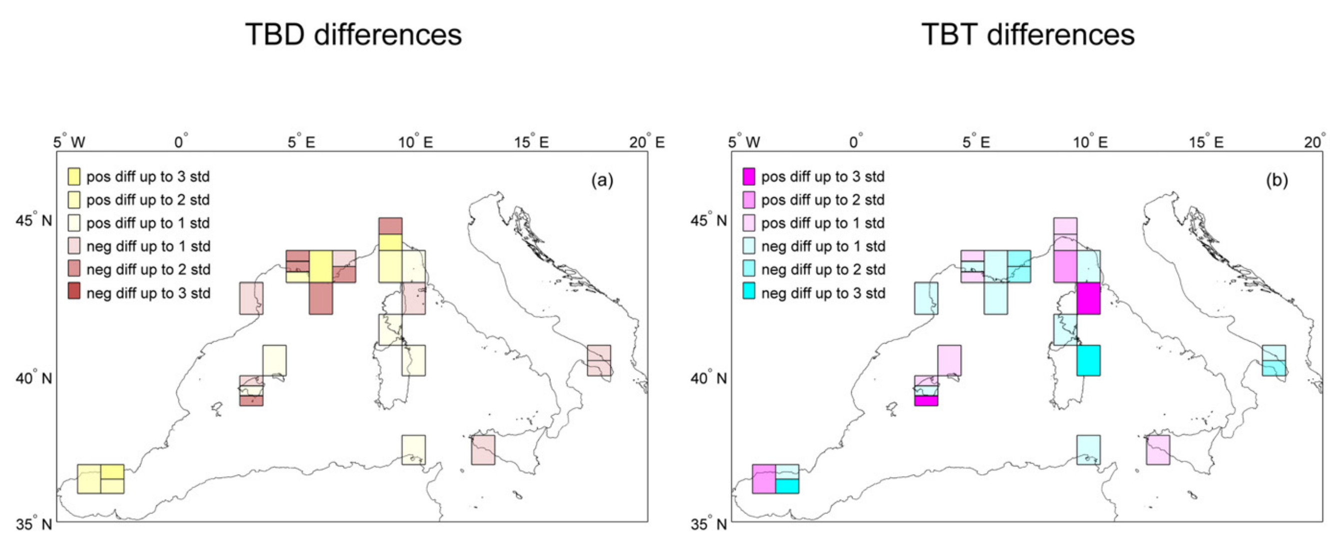

Fig. 12. Same as Fig. 8 except it shows TBD (a) and TBT (b).

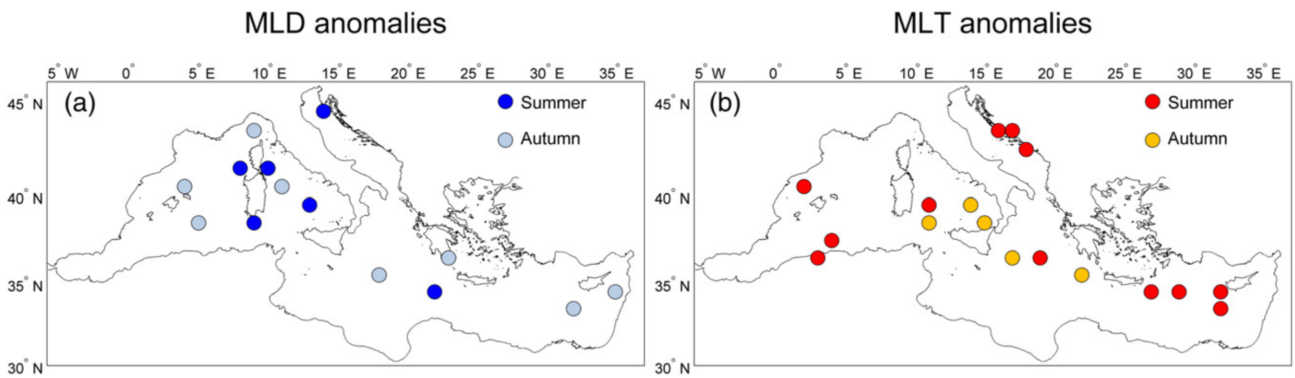

Fig. 13. Locations where the frequency of MLD positive anomalies (a) and of MLT positive anomalies (b) shows a 30% increase comparing the periods 1990–2011 and 1945–1965.

mortalities should be uniform. Fig. 9a and Fig. 9b show that this is not the case: both positive MLT and MLD anomalies are clearly more frequent (consistently with Table 2) during mass mortalities. The KS-test results show that the hypothesis of a uniform distribution can be rejected with a high (95%) confidence level and strongly support the effect of warm MLT and thick MLD anomalies (which together imply a higher heat content in the ML) on the observed mass mortalities.

Though this analysis shows a clear link in time and space between MLD and MLT anomalies and mass mortalities, the overall statistical distribution of MLD and MLT anomalies in the locations where mass mortalities have occurred during the analyzed 1945–2011 period has not changed. The KS-test has been carried out to compare the statistics of anomalies in the initial (1945–1965) and final (1990–2011) 20 year long periods and it shows that differences are not significant at any relevant confidence level (the distributions are shown in Fig. 10), though there is a mild indication that MLD/MLT were deeper/higher in the final 20 years.

A further detailed inspection of data shown in Figs. 4–7 shows that actually in these locations the MLD and MLT trends are not significant. Therefore, the link between the occurrence of mass mortalities of benthic invertebrates and MLD/MLT anomaly is a robust evidence of the critical environmental importance of the latter, but should be very cautiously used as evidences of local climate change, unless regular monitoring over a sufficiently long time can actually document the increased frequency of events.

However, at Mediterranean scale, the statistical distribution of summer and autumn MLT anomalies in the periods 1945–1965 and 1990–2011 are different with more frequent warm anomalies in the second period (Fig. 11). According to the KS-test differences are significant at the 99% and 95% level in summer and autumn, respectively, providing an evidence of a shift of MLT towards warmer conditions in the whole Mediterranean Sea (it is worth noticing that such a behavior, even though limited to sea surface temperature, had been shown by Marullo et al., 2011). No analogous change is evident for MLD. In conclusion, it is evident with a high level of confidence that warm MLT anomalies have become more frequent with respect to the mid-20th century, though this is not the case in the locations where mass mortalities have been reported.

A similar investigation has been performed on the association of mass mortalities and thermocline base parameters TBD and TBT. In fact, there are widespread significant trends of TBD and TBT, and the thermocline base parameters show a general deepening and cooling of the entire Mediterranean basin over the period of observations (Figs. 6 and 7). However, when the focus is on mass mortalities, no clear association is found. Fig. 12, which is the analogous of Fig. 8 but for TBD and TBT, shows that for these two parameters no dominant pattern can be identified in coincidence with the observed mass mortalities. The conclusion is that the evolution TBT and TBD has no significant influence on the temporal and spatial distribution of the mortality events considered in this study.

5. Conclusions

In the Mediterranean Sea, considering the period 1945–2011, there is a consistent picture of a progressively thicker and warmer ML, suggesting that heat penetration inside the upper portion of the water column has intensified in the last decades of the analyzed period.

This robust conclusion on the past behavior of the ML can be the basis for a further study on the meteorological characterization of the Mediterranean Sea climate change patterns. Warmer and thicker ML indicates that warming and stronger mixing are occurring simultaneously over most of the Mediterranean Sea, which is an unusual combination suggesting a possibly complex effect of climate change on air–sea interaction. The ML in spring shows, on the contrary, cooling and deepening, except in the Ionian and Balearic Seas, suggesting progressively stronger winds increasing its thickness and decreasing its temperature. The Aegean Sea presents a distinguished behavior with respect to the rest of the Mediterranean Sea with cooling and deepening in all seasons. All these features indicate the importance of a future study devoted to the understanding of the changing meteorological regimes causing these features and their spatial patterns.

This study provides clear statistical evidence that large positive MLD and MLT anomalies are associated with mass mortalities. Most mass mortalities occurred when the ML was deeper and warmer than average, so that the hypothesis that MLD and MLT have no influence on mass mortalities events can be rejected at a 95% confidence level.

In the past, two main drivers of biodiversity distribution have been identified, namely light (Pérès and Picard, 1964), and water movement (Riedl, 1971). This study shows the sensitivity of significant components of the Mediterranean Sea benthos to the vertical temperature profile, as well.

At the locations where mortalities have been reported, the frequency of warmer ML has not changed in the period 1990–2011 with respect to 1945–1965. This suggests that mass mortalities should be cautiously used as evidences of climate change, though they are associated to positive temperature extremes. In fact, irregular monitoring practice can strongly affect the results suggesting faking trends in the actual occurrence of mass mortalities.

However, at Mediterranean basin scale positive MLT anomalies have become more frequent and it is plausible to think that lack of data and regular reporting practice have prevented so far a more widespread evidence of mass mortalities than it has been reported in the scientific literature. Therefore, the lack of a systematic strategy for ecosystem monitoring and threshold identification is a major issue for this analysis and a plan for its implementation at basin scale is required. On the one hand, insufficient monitoring might have falsely suggested changing environmental condition at locations that have not been significantly affected by climate change. On the other hand, it might have prevented identifying a likely ongoing environmental change associated with climate change at basin scale.

Cells where frequency of MLD and MLT positive anomalies have increased by more than 30% in the period 1990–2011 with respect to 1945–1965 are shown in Fig. 13. These are suggested “hot spots” where a dedicated investigation is likely to find evidences of changing environmental conditions in coastal ecosystems. The subset of these locations that are in proximity of the coastline are suggested by this study for pilot campaigns and data rescue initiatives for identifying early warnings of climate change impacts on the Mediterranean marine ecosystems.

Acknowledgements

This study was partly funded by the Centro Euro Mediterraneo sui Cambiamenti Climatici. The research leading to these results received financial support from the Italian flagship project RItMare. The research also received funding from the European Community's 7th Framework Programmes (FP7/2007–2013) for the project COCONET (Grant agreement No. 287844) and PERSEUS (Grant agreement No. 287600).

Appendix A

A.1. The threshold method (THR)

The threshold method is a very commonly employed technique to derive the MLD, because it is simple and it can be applied to profiles with a great variety of vertical resolutions. Advantages of this method with respect to others have been shown in previous studies (Thomson and Fine, 2003; Brainerd and Gregg, 1995).

The MLD is defined as the minimum depth at which the (negative) temperature difference with respect to the surface value crosses a prescribed threshold (de Boyer Montègut et al., 2004). Given the temperature profile $T(z)$ as function of depth z, its value T_i linearly interpolated at the depth z_i (with $z_i = z_0 - i\Delta z$, where z_0 is a reference depth, $\Delta z = 1$ m), $T_0 = T(z_0)$, λ a the chosen threshold value, the lowest index j such that $T_j - T_0 \leq -\lambda$,

is found. The MLD is determined by linear interpolation between z_j and z_{j-1} as the depth z_{MLD} of so that:

$$T(z_{MLD}) - \mathrm{T}_0 = \lambda.$$

Results depend on the choice of the reference level z_0 and of the threshold value λ. In this study the reference depth z_0 is set at 10 m to avoid considering the uppermost part of the water column, which is affected by the diurnal cycle of warming and cooling, and by some noise due to the instrument introduction in the water. The chosen threshold value is 0.2 °C, as it has been used by D'Ortenzio et al. (2005) in a climatology study of the mixed layer depth in the Mediterranean Sea.

A.2. Curvature-based criterion (CUR)

Recently, Lorbacher et al. (2006) developed an algorithm that estimates the MLD from observed temperature profiles based on the their second derivative, or “curvature”. With respect to the threshold method, the curvature criterion is less dependent on the choice of parameters, such as the surface reference value and the threshold value, and it can be applied to a large variety of cases. It determines the MLD based as the shallowest depth where a maximum curvature value occurs.

Given the vertical temperature profile, its gradient g_i at the level i are defined as:

$$g_i = \frac{T_i - T_{i=5\ \mathrm{m}}}{z_i - z_{i=5\ \mathrm{m}}},$$

where $i = 5$ m refers to the next level that is at least 5 m deeper than the level i. The curvature c_i is calculated as:

$$c_i = \frac{g_i - g_{i=1}}{z_{i-1} - z_i}.$$

This algorithm depends on the choice of some parameters and boundary conditions (see Lorbacher et al., 2006 for a detailed description of this method).

A.3. Three segments profile model (3SEG)

The three segments profile model approximates the temperature with three joint segments: the uppermost and the lowermost have constant T values, which approximate the temperature of the surface MLT and of the underlying deep layer, respectively (TBT). The whole vertical structure is therefore summarized by 4 parameters: 1) the temperature of the uppermost segment, which is the MLT, 2) the depth that it reaches, which is actually the MLD, 3) the temperature at the basis of the thermocline TBT, and 4) the depth where the deep layer begins (which is the TBD). The four parameter values defining the three segments are determined by an optimization procedure that minimizes the root mean square error of the idealized profile with respect to the observations. This procedure captures the MLD, the MLT, the TBD and the TBT.

A.4. Split and merge algorithm (SM)

The split and merge method fits an arbitrary number joint line segments to the temperature profile and it can be considered a generalization of the 3SEG model. It was developed by Pavlidis and Horowitz (1974) to estimate the optimal decomposition of plane curves and waveforms and it was successively used by Thomson and Fine (2003) to detect the MLD and other upper ocean features from hydrographic profiles data.

This algorithm fits the standardized temperature–depth profile with piecewise polynomial functions by an iterative adjustment procedure. Given the observed set of values z_i, T_i, the algorithm seeks the minimum number of segments n that approximate the profile such that the error norm between segment and observed profile is less than a specified threshold. The split and merge iteration eventually merges adjacent segments with similar coefficients and splits those segments with a error norm above the specified threshold (0.01 in this study).

Thomson and Fine (2003) found a slight improvement in estimates of the “true” MLD using their method compared with other temperature threshold methods for the continental margin waters of British Columbia, and suggested that the method might be used to “simultaneously determine other structural features of the upper ocean” such as the thermocline depth. This method generally works well, though sometimes detects a “mixed layer bottom” beneath a surface layer with significant vertical gradient of temperature (Thomson and Fine, 2003).

A.5. Variable representative isotherm method (ISO)

A widely used and operationally very simple alternative to the criteria described above is to use reference MLTs and TBTs, computed separately for each season. Here, we have used the procedure described by Pizarro and Montecinos (2004) and considered the mean seasonal temperature profile. As MLD reference we have chosen, starting from the surface, the depth with the largest temperature gradient. As TBD reference, we have selected the minimum depth below the mixed layer where the gradient is smaller than 0.03 °C m^{-1}. Temperatures associated to these depths in the mean temperature profiles (MLT and TBT references) are used as references for the analysis of individual temperature profiles. The MLD and TBD of each profile are the depth at which its temperature matches the reference MLT and TBT values, respectively. The method can fail if temperatures along the profile are colder than the reference MLT.

Table A.1
List of procedures for the analysis of the upper column considered in this study:

VIS	VISual	Subjective visual estimate of profile structure
THR	THReshold	MLD is defined as the minimum depth at which the (negative) temperature difference with respect to the surface value crosses a prescribed threshold
CUR	CURvature	MLD is estimated as the shallowest depth with maximum curvature value
3SEG	3 SEGments	The temperature profile is represented with three joint segments: mixed layer, thermocline, deep layer
SM	Split and merge	An arbitrary number of joint line segments are used to fit the temperature profile
ISO	ISOtherm	MLD and TBD are estimated on the basis of reference MLT and TBT values

Appendix B

B.1. Application of the 3SEG method on temperature profiles collected at DYFAMED station

Fig. 1B shows the application of the 3SEG method on temperature profiles collected at DYFAMED station in July (Fig. 1Ba, b), in August (Fig. 1Bc, d) and in September (Fig. 1Be, f). Fig. 1Bb, d, f shows the results of the 3SEG method at the beginning (dark blue) and end (light blue) of the analyzed time series, respectively for July, August and September. MLD, MLT, TBD and TBT used in Fig. 1Bb, d, f represent the initial and final values of the linear regression best fits to the respective time series.

References

Alexander, M.A., Timlin, M.S., Scott, J.D., 2001. Winter-to-winter recurrence of sea surface temperature, salinity and mixed layer depth anomalies. Prog. Oceanogr. 49 (1), 41–61.

Babu, K.N., Sharma, R., Agarwal, N., Agarwal, V.K., Weller, R.A., 2004. Study of the mixed layer depth variations within the north Indian Ocean using a 1-D model. J. Geophys. Res.-Oceans 109 (C8). http://dx.doi.org/10.1029/2003JC002024.

Bensoussan, N., Romano, J.-C., Harmelin, J.-G., Garrabou, J., 2010. High resolution characterization of northwest Mediterranean coastal waters thermal regimes: to better understand responses of benthic communities to climate change. Estuar. Coast. Shelf S. 87 (3), 431–441. http://dx.doi.org/10.1016/j.ecss.2010.01.008.

Bernardello, R., Cardoso, J.G., Bahamon, N., et al., 2012. Factors controlling interannual variability of vertical organic matter export and phytoplankton bloom dynamics — a numerical case-study for the NW Mediterranean Sea. Biogeosciences 9 (11), 4233–4245. http://dx.doi.org/10.5194/bg-9-4233-2012.

Bindoff, N.L., Willebrand, J., Artale, V., et al., 2007. Observations: oceanic climate change and sea level. In: Solomon, S., Qin, D., Manning, M., Chen, Z., Marquis, M., Averyt, K.B., Tignor, M., Miller, H.L. (Eds.), Climate Change 2007: The Physical Science Basis. Contribution of Working Group I to the Fourth Assessment Report of the Intergovernmental Panel on Climate Change. Cambridge University Press, Cambridge, United Kingdom and New York, NY, USA.

Brainerd, K.E., Gregg, M.C., 1995. Surface mixed and mixing layer depths. Deep-Sea Res. Pt I 42 (9), 1521–1543.

Cebrian, E., Jesus Uriz, M., Garrabou, J., Ballesteros, E., 2011. Sponge mass mortalities in a warming Mediterranean Sea: are cyanobacteria-harboring species worse off? PLoS One 6 (6). http://dx.doi.org/10.1371/journal.pone.0020211.

Cerrano, C., Bavestrello, G., Bianchi, C.N., et al., 2000. A catastrophic mass-mortality episode of gorgonians and other organisms in the Ligurian Sea (Northwestern Mediterranean), summer 1999. Ecol. Lett. 3 (4), 284–293. http://dx.doi.org/10.1046/j.1461-0248.2000.00152.x.

Chen, D., Busalacchi, A.J., Rothstein, L.M., 1994. The roles of vertical mixing, solar-radiation, and wind stress in a model simulation of the sea-surface temperature seasonal cycle in the Tropical Pacific-Ocean. J. Geophys. Res.-Oceans 99 (C10), 20345–20359. http://dx.doi.org/10.1029/94JC01621.

Chu, P.C., Fralick, C.R., Haeger, S.D., Carron, M.J., 1997. A parametric model for the Yellow Sea thermal variability. J. Geophys. Res.-Oceans 102 (C5), 10499–10507. http://dx.doi.org/10.1029/97JC00444.

Coma, R., Ribes, M., Serrano, E., et al., 2009. Global warming-enhanced stratification and mass mortality events in the Mediterranean. P. Natl. Acad. Sci. USA 106 (15), 6176–6181. http://dx.doi.org/10.1073/pnas.0805801106.

de Boyer Montègut, C., Madec, G., Fischer, A.S., Lazar, A., Iudicone, D., 2004. Mixed layer depth over the global ocean: an examination of profile data and a profile-based climatology. J. Geophys. Res.-Oceans 109. http://dx.doi.org/10.1029/2004JC002378 (C12).

Deser, C., Alexander, M.A., Timlin, M.S., 1996. Upper-ocean thermal variations in the North Pacific during 1970–1991. J. Clim. 9 (8), 1840–1855.

Dommenget, D., Latif, M., 2002. Analysis of observed and simulated SST spectra in the midlatitudes. Clim. Dyn. 19 (3–4), 277–288. http://dx.doi.org/10.1007/s00382-002-0229-9.

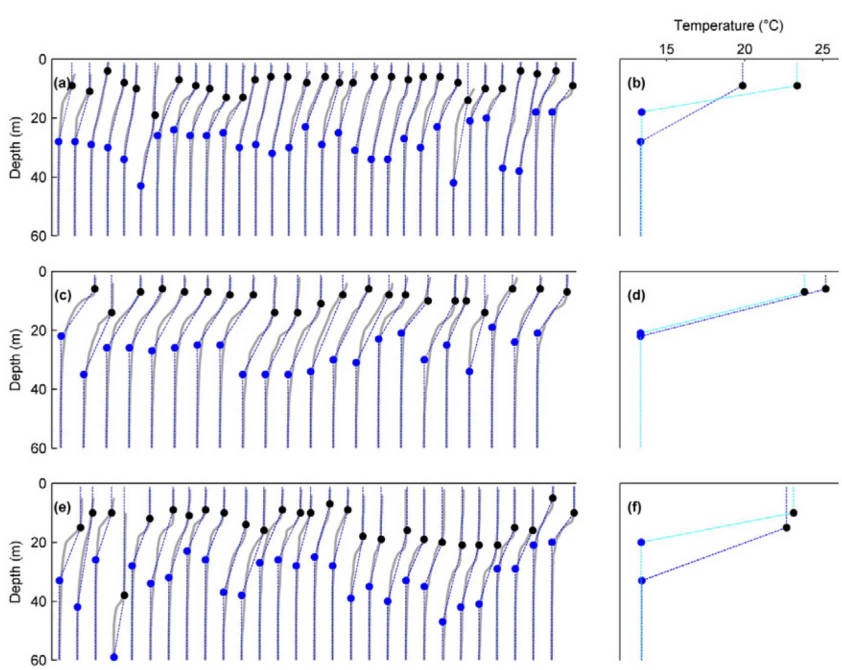

Fig. 1B. Results of the 3SEG method on temperature profiles collected at DYFAMED station for July (a, b), August (c, d) and September (e, f). The panels b, d, f show the initial (dark blue) and final (light blue) temperature profile of the analyzed periods based on linear interpolation of the time series of the parameters describing the ML.

Dong, S., Garzoli, S.L., Baringer, M., 2009. An assessment of the seasonal mixed layer salinity budget in the Southern Ocean. J. Geophys. Res.-Oceans 114. http://dx.doi.org/10.1029/2008JC005258.

Donguy, J.R., Meyers, G., 1987. Observed and modeled topography of the 20-degrees-C isotherm in the Tropical Pacific. Oceanol. Acta 10 (1), 41–48.

D'Ortenzio, F., Iudicone, D., de Boyer Montègut, C., et al., 2005. Seasonal variability of the mixed layer depth in the Mediterranean Sea as derived from in situ profiles. Geophys. Res. Lett. 32 (12). http://dx.doi.org/10.1029/2005GL022463.

D'Ortenzio, F., Antoine, D., Marullo, S., 2008. Satellite-driven modeling of the upper ocean mixed layer and air–sea CO_2 flux in the Mediterranean Sea. Deep-Sea Res. Pt I 55 (4), 405–434. http://dx.doi.org/10.1016/j.dsr.2007.12.008.

Fichaut, M., Garcia, M.J., Giorgetti, A., et al., 2003. MEDAR/MEDATLAS 2002: a Mediterranean and Black Sea database for the operational Oceanography. In: Dahlin, H., et al. (Eds.), Building the European Capacity in Operational Oceanography: Proceedings of the 3rd International Conference on EuroGOOS 3–6 December 2002, Athens, Greece. Elsevier Oceanography Series Vol. 69, pp. 645–648.

Freeland, H.J., 2013. Evidence of change in the winter mixed layer in the Northeast Pacific Ocean: a problem revisited. Atmosphere-Ocean 51 (1), 126–133. http://dx.doi.org/10.1080/07055900.2012.754330.

Gardner, W.D., Chung, S.P., Richardson, M.J., Walsh, I.D., 1995. The oceanic mixed-layer pump. Deep-Sea Res. Pt II 42 (2), 757–775.

Garrabou, J., Coma, R., Bensoussan, N., et al., 2009. Mass mortality in Northwestern Mediterranean rocky benthic communities: effects of the 2003 heat wave. Glob. Chang. Biol. 15 (5), 1090–1103. http://dx.doi.org/10.1111/j.1365-2486.2008.01823.x (al.).

Hanawa, K., Sugimoto, S., 2004. 'Reemergence' areas of winter sea surface temperature anomalies in the world's oceans. Geophys. Res. Lett. 31 (10). http://dx.doi.org/10.1029/2004GL019904.

Heimburger, L.-E., Lavigne, H., Migon, C., et al., 2013. Temporal variability of vertical export flux at the DYFAMED time-series station (Northwestern Mediterranean Sea). Prog. Oceanogr. 119, 59–67. http://dx.doi.org/10.1016/j.pocean.2013.08.005.

Holte, J., Talley, L., 2009. A new algorithm for finding mixed layer depths with applications to Argo DATA and Subantarctic mode water formation. J. Atmos. Ocean. Technol. 26 (9), 1920–1939. http://dx.doi.org/10.1175/2009JTECHO543.1.

Huete-Stauffer, C., Vielmini, I., Palma, M., et al., 2011. *Paramuricea clavata* (Anthozoa, Octocorallia) loss in the Marine Protected Area of Tavolaria (Sardinia, Italy) due to a mass mortality event. Mar. Ecol. 32, 107–116. http://dx.doi.org/10.1111/j.1439-0485.2011.00429.x.

Johnson, D.R., Garcia, H.E., Boyer, T.P., 2013. World Ocean Database 2013 Tutorial. Sydney Levitus, Ed.; Alexey Mishonov, Technical Ed.; NODC Internal Report 23, NOAA Printing Office, Silver Spring, MD. 25 p. Available at http://www.nodc.noaa.gov/OC5/WOD13/docwod13.html.

Kara, A.B., Rochford, P.A., Hurlburt, H.E., 2000. An optimal definition for ocean mixed layer depth. J. Geophys. Res.-Oceans 105 (C7), 16803–16821. http://dx.doi.org/10.1029/2000JC900072.

Kara, A.B., Rochford, P.A., Hurlburt, H.E., 2003. Mixed layer depth variability over the global ocean. J. Geophys. Res.-Oceans 108 (C3). http://dx.doi.org/10.1029/2000JC000736.

Kara, A.B., Helber, R.W., Wallcraft, A.J., 2010. Evaluations of threshold and curvature mixed layer depths by various mixing schemes in the Mediterranean Sea. Ocean Model. 34 (3–4), 166–184. http://dx.doi.org/10.1016/j.ocemod.2010.05.006.

Kessler, W.S., 1990. Observations of long Rossby waves in the northern Tropical Pacific. J. Geophys. Res.-Oceans 95 (C4), 5183–5217. http://dx.doi.org/10.1029/JC095iC04p05183.

Kessler, W.S., McPhaden, M.J., Weickmann, K.M., 1995. Forcing of intraseasonal Kelvin waves in the Equatorial Pacific. J. Geophys. Res.-Oceans 100 (C6), 10613–10631. http://dx.doi.org/10.1029/95JC00382.

Lavigne, H., D'Ortenzio, F., Migon, C., et al., 2013. Enhancing the comprehension of mixed layer depth control on the Mediterranean phytoplankton phenology. J. Geophys. Res.-Oceans 118 (7), 3416–3430. http://dx.doi.org/10.1002/jgrc.20251.

Linares, C., Coma, R., Diaz, D., et al., 2005. Immediate and delayed effects of a mass mortality event on gorgonian population dynamics and benthic community structure in the NW Mediterranean Sea. Mar. Ecol. Prog. Ser. 305, 127–137. http://dx.doi.org/10.3354/meps305127.

Lopes, R.H.C., 2011. Kolmogorov–Smirnov Test. In: International Encyclopedia of Statistical Science. Springer, Berlin Heidelberg, pp. 718–720.

Lorbacher, K., Dommenget, D., Niiler, P.P., Kohl, A., 2006. Ocean mixed layer depth: a subsurface proxy of ocean-atmosphere variability. J. Geophys. Res.-Oceans 111 (C7). http://dx.doi.org/10.1029/ 2003JC002157.

Manzella, G.M.R., Reseghetti, F., Coppini, G., et al., 2007. The improvements of the ships of opportunity program in MFS-TEP. Ocean Sci. 3 (2), 245–258. http://dx.doi.org/10.5194/osd-3-1717-2006.

Marullo, S., Artale, V., Santoleri, R., 2011. The SST multidecadal variability in the Atlantic–Mediterranean region and its relation to AMO. J. Clim. 24 (16), 4385–4401. http://dx.doi.org/10.1175/2011JCLI3884.1.

Meyers, G., 1979a. Annual variation in the slope of the 14 °C isotherm along the equator in the Pacific Ocean. J. Phys. Oceanogr. 9, 885–891. http://dx.doi.org/10.1175/1520-0485(1979)009<0885:AVITSO>2.0.CO;2.

Meyers, G., 1979b. On the annual Rossby wave in the tropical North Pacific Ocean. J. Phys. Oceanogr. 9, 663–674. http://dx.doi.org/10.1175/1520-0485(1979)009<0663:OTARWI>2.0.CO;2.

Monterey, G., Levitus, S., 1997. Seasonal variability of mixed layer depth for the world ocean. NOAA Atlas NESDIS 14. 100 pp.Natl. Oceanic and Atmos. Admin.Silver Spring, Md

Ohlmann, J.C., Siegel, D.A., Gautier, C., 1996. Ocean mixed layer radiant heating and solar penetration: a global analysis. J. Clim. 9 (10), 2265–2280. http://dx.doi.org/10.1175/1520-0442(1996)009<2265:OMLRHA>2.0.CO;2.

Pavlidis, T., Horowitz, S.L., 1974. Segmentation of plane curves. Comput. IEEE Trans. 23 (8), 860–870. http://dx.doi.org/10.1109/T-C.1974.224041.

Pérès, J.M., Picard, J., 1964. Nouveau manuel de bionomie benthique de la Mer Méditerranée. Recueil des Travaux de la Station Marine d'Endoume Vol. 31, pp. 1–137.

Pizarro, O., Montecinos, A., 2004. Interdecadal variability of the thermocline along the west coast of South America. Geophys. Res. Lett. 31 (20). http://dx.doi.org/10.1029/2004GL020998.

Polovina, J.J., Mitchum, G.T., Evans, G.T., 1995. Decadal and basin-scale variation in mixed layer depth and the impact on biological production in the Central and North Pacific, 1960-88. Deep-Sea Res. Pt I 42 (10), 1701–1716. http://dx.doi.org/10.1016/0967-0637(95)00075-H.

Riedl, R., 1971. Water movement: general introduction. In: O., Kinne (Ed.), Marine Ecology. Wiley, London, pp. 1086–1088.

Rivetti, I., Fraschetti, S., Lionello, P., Zambianchi, E., Boero, F., 2014. Global warming and mass mortalities of benthic invertebrates in the Mediterranean Sea. PLoS One 9 (12). http://dx.doi.org/10.1371/journal.pone.0115655.

Ruiz, S., Renault, L., Garau, B., Tintore, J., 2012. Underwater glider observations and modeling of an abrupt mixing event in the upper ocean. Geophys. Res. Lett. 39. http://dx.doi.org/10.1029/2011GL050078.

Sharp, D.G., McLain, D.R., 1993. Fisheries, El Niño–Southern Oscillation and upper-ocean temperature records: an eastern Pacific example. Oceanography 6 (1), 13–22.

Suga, T., Motoki, K., Aoki, Y., Macdonald, A.M., 2004. The North Pacific climatology of winter mixed layer and mode waters. J. Phys. Oceanogr. 34 (1), 3–22. http://dx.doi.org/10.1175/1520-0485(2004)034<0003:TNPCOW>2.0.CO;2.

Taillandier, V., D'Ortenzio, F., Antoine, D., 2012. Carbon fluxes in the mixed layer of the Mediterranean Sea in the 1980s and the 2000s. Deep-Sea Res. Pt I 65, 73–84. http://dx.doi.org/10.1016/j.dsr.2012.03.004.

Thomson, R.E., Fine, I.V., 2003. Estimating mixed layer depth from oceanic profile data. J. Atmos. Ocean. Technol. 20 (2), 319–329. http://dx.doi.org/10.1175/1520-0426(2003)020<0319:EMLDFO>2.0.CO;2.

Vidussi, F., Claustre, H., Manca, B.B., Luchetta, A., Marty, J.C., 2001. Phytoplankton pigment distribution in relation to upper thermocline circulation in the eastern Mediterranean Sea during winter. J. Geophys. Res.-Oceans 106 (C9), 19939–19956. http://dx.doi.org/10.1029/1999JC000308.

Wang, B., Wu, R.G., Lukas, R., 2000. Annual adjustment of the thermocline in the tropical Pacific Ocean. J. Clim. 13 (3), 596–616. http://dx.doi.org/10.1175/1520-0442(2000)013<0596:AAOTTI>2.0.CO;2.

Yasuda, I., Watanabe, T., 2007. Chlorophyll a variation in the Kuroshio Extension revealed with a mixed-layer tracking float: implication on the longterm change of Pacific saury (*Cololabis saira*). Fish. Oceanogr. 16 (5), 482–488. http://dx.doi.org/10.1111/j.1365-2419.2007.00457.x.

Zawada, D.G., Zaneveld, J.R.V., Boss, E., et al., 2005. A comparison of hydrographically and optically derived mixed layer depths. J. Geophys. Res.-Oceans 110 (C11). http://dx.doi.org/10.1029/2004JC002417.